1-1-2010

Easy preparation of SnO2@carbon composite nanofibers with improved lithium ion storage properties

Zhixin Chen
University of Wollongong, zchen@uow.edu.au

Zaiping Guo
University of Wollongong, zguo@uow.edu.au

Hua-Kun Liu
University of Wollongong, hua@uow.edu.au

Guodong Du
gd616@uow.edu.au

Xuebin Yu
xyu@uow.edu.au

See next page for additional authors

Easy preparation of SnO2@carbon composite nanofibers with improved lithium ion storage properties

Abstract

SnO2@carbon nanofibers were synthesized by a combination of electrospinning and subsequent thermal treatments in air and then in argon to demonstrate their potential use as an anode material in lithium ion battery applications. The as-prepared SnO2@carbon nanofibers consist of SnO2 anoparticles/ nanocrystals encapsulated in a carbon matrix and contain many mesopores. Because of the charge pathways, both for the electrons and the lithium ions, and the buffering function provided by both the carbon encapsulating the SnO2 nanoparticles and the mesopores, which tends to alleviate the volumetric effects during the charge/discharge cycles, the nanofibers display a greatly improved reversible capacity of 420 mAh/g after 100 cycles at a constant current of 100 mA/g, and a sharply enhanced reversible capacity at higher rates (0.5, 1, and 2 C) compared with pure SnO2 nanofibers, which makes it a promising anode material for lithium ion batteries.

Keywords

Easy, preparation, SnO2, carbon, composite, nanofibers, improved, lithium, ion, storage, properties

Disciplines

Arts and Humanities | Life Sciences | Medicine and Health Sciences | Social and Behavioral Sciences

Publication Details

Yang, Z., Du, G., Guo, Z., Yu, X., Chen, Z., Zhang, P., Chen, G. & Liu, H. K. (2010). Easy preparation of SnO2@carbon composite nanofibers with improved lithium ion storage properties. Journal of Materials Research, 25 (8), 1516-1524.

Authors

Zhixin Chen, Zaiping Guo, Hua-Kun Liu, Guodong Du, Xuebin Yu, Guonan Chen, Peng Zhang, and Zunxian Yang

Easy preparation of SnO_2@carbon composite nanofibers with improved lithium ion storage properties

Zunxian Yang
Institute for Superconducting and Electronic Materials, University of Wollongong, Wollongong, NSW 2522, Australia; and Institute of Micro/Nano-Sensors & Solar Energy Cells, Fuzhou University, Fuzhou 350108, People's Republic of China

Guodong Du
Institute for Superconducting and Electronic Materials, University of Wollongong, Wollongong, NSW 2522, Australia

Zaiping Guo[a)]
Institute for Superconducting and Electronic Materials, and School of Mechanical, Materials and Mechatronics Engineering, University of Wollongong, Wollongong, NSW 2522, Australia

Xuebin Yu
Institute for Superconducting and Electronic Materials, University of Wollongong, Wollongong, NSW 2522, Australia; and Department of Materials Science, Fudan University, Shanghai 200433, People's Republic of China

Zhixin Chen
School of Mechanical, Materials and Mechatronics Engineering, University of Wollongong, Wollongong NSW 2522, Australia

Peng Zhang
Institute for Superconducting and Electronic Materials, University of Wollongong, Wollongong, NSW 2522, Australia

Guonan Chen
Key Laboratory of Analysis and Detection Technology for Food Safety of the Ministry of Education, Fuzhou University, Fuzhou 350002, People's Republic of China

Huakun Liu
Institute for Superconducting and Electronic Materials, University of Wollongong, Wollongong, NSW 2522, Australia

(Received 30 December 2009; accepted 15 March 2010)

SnO_2@carbon nanofibers were synthesized by a combination of electrospinning and subsequent thermal treatments in air and then in argon to demonstrate their potential use as an anode material in lithium ion battery applications. The as-prepared SnO_2@carbon nanofibers consist of SnO_2 nanoparticles/nanocrystals encapsulated in a carbon matrix and contain many mesopores. Because of the charge pathways, both for the electrons and the lithium ions, and the buffering function provided by both the carbon encapsulating the SnO_2 nanoparticles and the mesopores, which tends to alleviate the volumetric effects during the charge/discharge cycles, the nanofibers display a greatly improved reversible capacity of 420 mAh/g after 100 cycles at a constant current of 100 mA/g, and a sharply enhanced reversible capacity at higher rates (0.5, 1, and 2 C) compared with pure SnO_2 nanofibers, which makes it a promising anode material for lithium ion batteries.

I. INTRODUCTION

Many metal oxides,[1–4] as promising anode materials for lithium ion batteries, have attracted considerable attention as their high capacity compares with that of graphite (372 mAh/g).[5,6] Among those metal oxides, tin dioxide has attracted particular interest because of its high capacity (781 mAh/g).[6] Nevertheless, practical implementation of SnO_2 in lithium-ion batteries is greatly frustrated by the large initial irreversible capacity induced by Li_2O formation and the abrupt capacity fading caused by volume variation (up to 258%[7]). Myriad charge transport and electronic conduction issues[8] have been attributed to these factors, and they have turned out to be major obstacles that militate against any practical use of SnO_2. There may be two basic solutions to alleviate this problem: one generally accepted strategy is to

[a)]Address all correspondence to this author.
e-mail: zguo@uow.edu.au
DOI: 10.1557/JMR.2010.0194

effectively disperse tin oxide in the form of nanoparticles into "buffering" matrices that may cushion the mechanical effects of the volume changes. Generally, carbonaceous materials can be the most effective candidates among the "buffering" matrices because of their good conductivity, Li^+ permeability, and chemical compatibility with tin oxide, the Li–Sn alloys, and the electrochemical system.[7] Another alternative strategy[9–11] is to prepare tin oxide in the form of nanostructured materials, especially one-dimensional nanomaterials, because of their adequate potential to enhance kinetic properties owing to their large surface area and short Li^+ diffusion length from a structural viewpoint.[8]

Therefore, viable SnO_2-based electrode materials mainly involve composite materials[12] and nanomaterials such as nanotubes,[5,13–15] nanowires,[16–19] hollow spheres,[20] mesoporous structures,[21] etc. These SnO_2-based nanomaterials are formed separately from the carbonaceous matrices in different steps[22] or prepared by a template method.[14,15] Some are very expensive because of the complicated process or the special starting material, while others cannot be classed as one-dimensional SnO_2@carbon matrices at all. Therefore, achieving one easy step to prepare tin oxide encapsulated in carbonaceous matrices with favorable one-dimensional nanostructured materials is challenging, but advantageous, not only for improving the conductivity, but also for alleviating the mechanical effects of the volume changes during the charge/discharge process.

Electrospinning is one simple method to form continuous one-dimensional nanofibers under the electrostatic force of the charges on the surface of a liquid droplet in a sufficiently high electric field, which is applied between the capillary nozzle and the metal collector.[23,24] Herein, this paper presents a relatively simple and low-cost approach to prepare SnO_2@carbon composite nanofibers by a combination of electrospinning and subsequent thermal treatments. In addition to combining the advantages of SnO_2 nanoparticles and carbon matrices, this SnO_2@carbon nanofiber composite has more unique advantages,[25] such as porosity, one-dimensional nanostructures, and large surface-to-volume ratio, and these have been investigated in a preliminary way with a view to its potential use as an anode material for the lithium ion batteries.

II. EXPERIMENTAL

A. Preparation of SnO_2@carbon nanofibers

The procedures for preparing the electrospinning solution have been described elsewhere[26] in detail. Simply, 0.7 g polyacrylonitrile (PAN; MW = 150,000, Aldrich, St. Louis, MO) was dissolved in 6.3 g N,N-dimethylformamide (DMF; 99.8%, Aldrich) at 80 °C with vigorous stirring for 2 h (solution No. 1). Then, 0.5 g tin(II) 2-ethylhexanoate (95%, Aldrich) was mixed with 2.5 g anhydrous ethanol (solution No. 2). Afterward, the No. 2 solution was added dropwise to the No. 1 solution at 80 °C with vigorous stirring. The mixed solution was then stirred at room temperature for 3 h again. The polymer solution was transferred into a 10 mL syringe with a capillary tip (0.8 mm diameter). For spinning, the setup was similar to that described previously.[24] Typically, the collector was placed 8 cm from the spinneret to collect the nanofibers. A high voltage of 13 kV was supplied at the spinneret by a direct-current power supply (DW-P303-5ACCD, Tianjin Dongwen High Voltage Power Supply Co., Tianjin, China). The solution was pushed out of the spinneret by a syringe pump (TS2-60, Baoding Lange Constant Flux Pump Co., Baoding, Heibei, China) at the rate of 0.5 mL/h. The collector was kept at 180 °C during electrospinning to evaporate the solvent. After spinning for more than 6 h, the nanofiber films were easily peeled off. The electrospun nanofibers were first partly pyrolyzed and carbonized in an air environment at 360 °C for 1 h (heating rate: less than 1 °C/min), and then fully carbonized at 500 °C for 2 h in argon atmosphere (heating rate: 2 °C/min). Finally, a black film (SnO_2@carbon nanofibers) was obtained.

B. Material characterization

The morphology was evaluated using a JEOL 7500FA field emission scanning electron microscope (FE–SEM; JEOL, Tokyo, Japan). Transmission electron microscope (TEM) investigations were performed using a JEOL 2011F analytical electron microscope (JEOL; Tokyo, Japan) operating at 200 kV. The composition and crystal structures of the SnO_2@carbon nanofibers were obtained by x-ray diffraction (XRD) analysis (MMA, GBC, Australia). Energy dispersive x-ray spectroscopy (EDX) analysis was carried out on the JEOL 7500FA analytical electron microscope as well. X-ray photoelectron spectroscopy (XPS) experiments were carried out on a VG Scientific ESCALAB 220IXL instrument using aluminum Kα x-ray radiation during XPS analysis. Raman spectroscopy was conducted on a Renishaw inVia Raman Microscope using the green light of an Ar laser (514 nm). Thermogravimetric analysis (TGA) of the PAN was carried out with a TGA/DSC1 type instrument (Mettler Toledo, Switzerland) at a heating rate of 10 °C/min from 25 to 1000 °C in argon.

C. Electrochemical characterization

Electrochemical evaluations were carried out using CR2032 coin cells. The working electrodes were formed by mixing the as-prepared SnO_2@carbon nanofibers, carbon black (Super P, MMM, Belgium), and poly(vinyl difluoride) (PVDF) at a weight ratio of 70:15:15 and pasting the mixture on copper foil. Pure lithium metal

was used for the counter and reference electrodes. The electrolyte consisted of a solution of 1 M/L LiPF6 in ethylene carbonate (EC)/dimethyl carbonate (DMC; 1:1, by volume) (Merck KgaA, Germany). Coin cells were assembled in a high-purity argon-filled glove box (Mbraun, Unilab, Germany). Charge and discharge were conducted at different current densities between cutoff potentials of 0.05 and 2.5 V. Cyclic voltammetry was performed on a PARSTAT–2273 electrochemical workstation.

III. RESULTS AND DISCUSSION

Uniform SnO_2@carbon nanofibers were simply synthesized by a combination of electrospinning and subsequent thermal treatments. The synthesis is based on a simple electrospinning method followed by pyrolysis and carbonization in an air environment and subsequently in an inert atmosphere. Specifically, the tin composite/PAN should be heated in an air environment at 360 °C for 1 h to adjust the content of carbon in the nanofibers (as the final carbon content in the nanofibers varies with the heating temperature and heating time). Further, they should be carbonized fully at 500 °C for 2 h in argon atmosphere to form SnO_2@carbon nanofibers consisting of SnO_2 nanoparticles encapsulated in the carbon. The final treatment temperature of the nanofibers was determined by the TGA results on the PAN (see the Appendix, Fig. A1).

Field emission scanning electron microscope images of the as-collected tin composite/PAN nanofibers and as-pyrolyzed SnO_2@carbon nanofibers at different magnifications are displayed in Fig. 1. Figure 1(a) shows a general overview of the uniform as-prepared tin composite/PAN nanofibers with lengths extending to several tens of millimeters. After calcination in air at 360 °C for 1 h and further in argon at 500 °C for 2 h, the nanofibrous morphology is maintained, as can be seen in Figs. A2(a)–A2(b) (see the Appendix) and Figs. 1(b)–1(d). The tin composite/PAN nanofibers have been transformed first to partly pyrolyzed and carbonized composite nanofibers with diameters of 80–120 nm, as shown in Fig. A2(a) and Fig. 1(b), and finally to fully carbonized thinner SnO_2@carbon nanofibers with diameters of 60–100 nm, consisting of SnO_2 nanoparticles encapsulated in carbon matrices, as shown in Fig. A2(b) and Figs. 1(c)–1(d), and their insets. To describe the formation of the SnO_2 nanoparticles in the SnO_2@carbon nanofibers, a high-magnification FE–SEM image of pure SnO_2 nanofibers, consisting of orderly bonded nanoparticles with an average size of ~10 nm, after calcination in air at 500 °C for 2 h, is also shown in Fig. A2(c). Thus, to some extent, the SnO_2@carbon nanofibers can be seen as an intermediate product in the preparation of pure SnO_2 nanofibers, but with carbon filling in between the SnO_2 particles in the

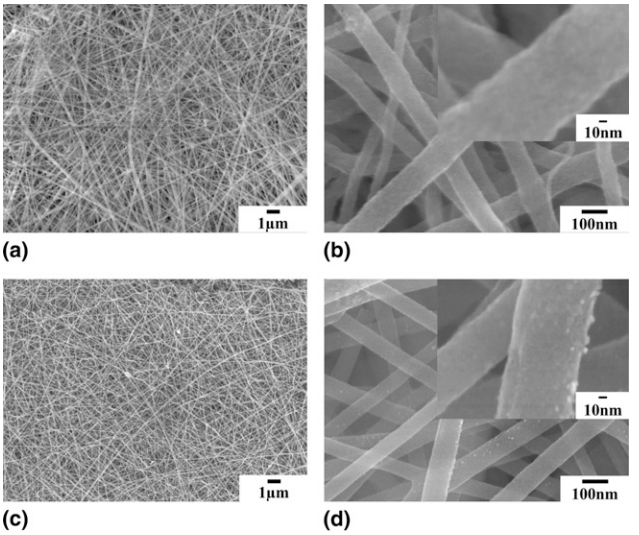

FIG. 1. FE–SEM images showing microstructures of as-collected tin composite/PAN nanofibers and as-pyrolyzed SnO_2@carbon nanofibers: (a) tin composite/PAN nanofibers; (b) as-pyrolyzed SnO_2 composite nanofibers in air at 360 °C for 1 h, and single nanofiber of SnO_2 composite (inset), at higher magnification; (c) as-pyrolyzed SnO_2@carbon nanofibers treated in air at 360 °C for 1 h and further in argon at 500 °C for 2 h; (d) as-pyrolyzed SnO_2@carbon nanofibers treated in air at 360 °C for 1 h and further in argon at 500 °C for 2 h, and single nanofiber of SnO_2@carbon (inset), at higher magnification.

SnO_2@carbon nanofibers. The carbon matrices can be oxidized (burnt off) in air under higher temperature for a longer time, leaving nanopores behind and forming structures similar to that of the pure SnO_2 nanofibers. However, the average size of the SnO_2 nanoparticles in the SnO_2@carbon nanofibers may differ from that in the pure SnO_2 nanofibers. Additionally, there are some fine SnO_2 nanoparticles on the outside of the SnO_2@carbon nanofibers, as shown in Fig. 1(d). Mesopores in the nanofiber films can be observed in high-magnification images of the nanofibers, as shown in Figs. 1(b) and 1(d). X-ray diffraction analysis of the as-pyrolyzed SnO_2@carbon nanofibers clearly reveals the diffraction pattern of a tetragonal rutile structure (JCPDS 41-1445) belonging to the space group $P4_2/mnm$ (136) with lattice parameters of $a = b = 4.7386$ Å and $c = 3.1872$ Å (Fig. 2). According to previous reports, carbothermal reduction of SnO_2 becomes feasible only when the carbonization temperature reaches around 600 °C,[20,27] and the XRD analysis (Fig. 2) confirms that carbothermal reduction of SnO_2 does not take place during carbonization at 500 °C.

Transmission electron microscope observation of the pyrolyzed SnO_2@carbon nanofibers provides worthwhile structural and chemical information (Fig. 3). Figure 3(a) displays the TEM bright-field image of a single SnO_2@carbon nanofiber, with the corresponding selected-area electronic diffraction (SAED) pattern [Fig. 3(a) inset] revealing the fine microstructure of

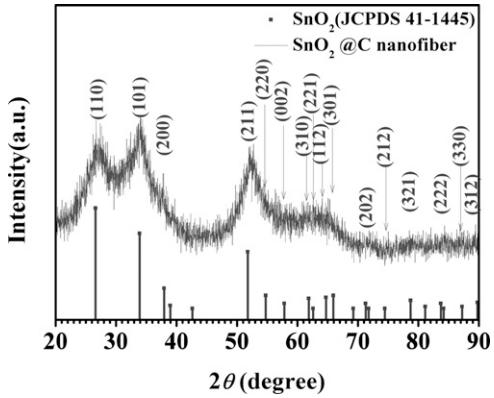

FIG. 2. X-ray diffraction pattern of as-prepared SnO_2@carbon nanofibers. The diffraction peaks indicate a tetragonal rutile structure for the SnO_2 (JCPDS 41-1445), as indexed in the pattern.

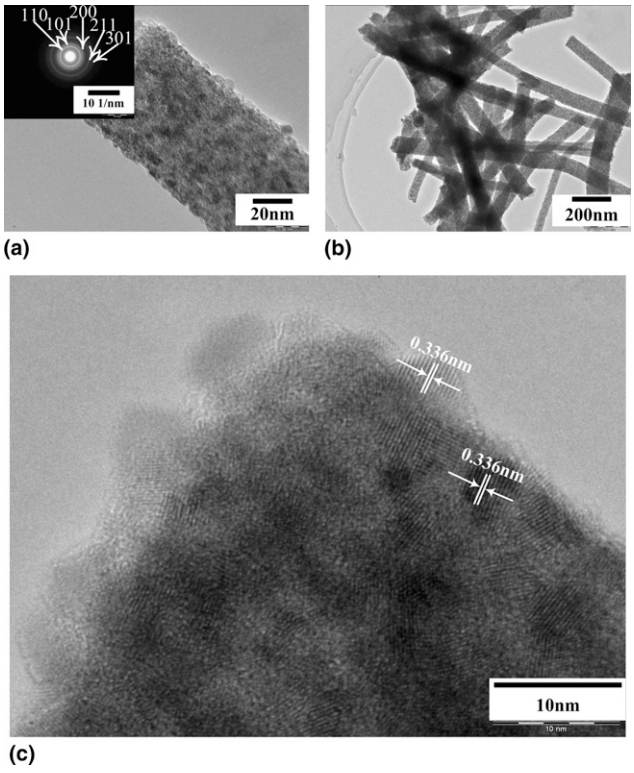

FIG. 3. (a) TEM image and SAED pattern (inset) of a SnO_2@carbon nanofiber. (b) Low-magnification TEM image of SnO_2@carbon nanofibers. (The image shows many hole/void nanopores between the bound SnO_2 nanoparticles in the nanofibers.) (c) HRTEM image of a section of a SnO_2@carbon nanofiber.

the SnO_2@carbon nanofibers. The ring-shaped SAED pattern indicates that the SnO_2 encapsulated in the SnO_2@carbon nanofibers is in polycrystalline form. The spotted diffraction rings from inside to outside can be indexed to the (110), (101), (200), (211), and (301) planes of rutile SnO_2, respectively [Fig. 3(a) inset]. These indexed patterns are in good agreement with the XRD results described previously. Combined with Fig. 3(a), the low-magnification TEM image in Fig. 3(b) of a few SnO_2@carbon nanofibers confirms that a SnO_2@carbon nanofiber consists of many small particles distributed in all the parts of the nanofiber. To further understand the structure of these nanoparticles encapsulated in the nanofibers, the high-resolution TEM (HRTEM) image [see Fig. 3(c)] clarifies the crystal structure, with an interplanar spacing revealed of approximately 0.336 nm between neighboring [110] planes of tetragonal SnO_2, as those planes were parallel to the electron beam. Only a few crystals have revealed clear lattice fringes in the HRTEM, while other areas without lattice fringes are present. These areas could be carbon-filled regions or crystals whose orientations are not parallel to the electron beam. It can be observed from Fig. 3(c) that, according to the grid area, the crystal size of the SnO_2 in the nanofibers is about 5–10 nm, and there are some crystals attached on the surface of the nanofiber. Figure 3 further confirms that those particles shown in both Figs. 3(a) and 3(b), except for those on the surface of the nanofibers, are actually SnO_2 crystals encapsulated in carbon matrices. Those SnO_2 nanoparticles originate from the decomposition and oxidation of tin(II) 2-ethylhexanoate in the tin composite/PAN nanofibers, followed by the further diffusion and crystal growth of tin dioxide in the nanofibers, similar to what has been reported previously.[28] The carbon matrices enveloping the SnO_2 nanoparticles in the nanofibers result from the pyrolysis and carbonization of PAN. Figure A3 (see the Appendix) reveals chemical information on the as-prepared SnO_2 nanofibers by means of energy-dispersive x-ray (EDX) spectra. The nanofibers mainly include the elements Sn, C, and O. Comparison of the carbon contents in the insets in Figs. A3(a) and A3(b) show that the heat treatment in argon at 500 °C led to an obvious decrease in carbon content from 18.53% to 12.08%, possibly due to a partial carbon burn-off and further pyrolysis of intermediate material at higher temperature according to the TGA result (Fig. A1). The results confirm that the SnO_2@carbon nanofibers consist of SnO_2 nanoparticles encapsulated in carbon matrices, and there are many mesopores between the nanofibers. This one-dimensional material would introduce unique advantages in lithium ion battery application[25] and could deliver significantly improved electrochemical performance compared with the pure SnO_2 nanofibers.[26]

The Raman spectra of the as-prepared SnO_2@carbon nanofibers are shown in Fig. A4 (see the Appendix). To investigate the properties of SnO_2 and carbon in SnO_2@carbon nanofibers more effectively, the two characteristic bands of SnO_2 and carbon are presented in Figs. A4(a) and A4(b), respectively. In Fig. A4(a), three Raman spectrum peaks for the SnO_2 can be observed at 471.49, 616.4, and 770.49 cm^{-1}, corresponding to the Eg, A1g, and B2g vibration modes, respectively.[17,29,30] These peaks demonstrate typical features of the rutile structure of the SnO_2. Compared with the Raman results

on SnO_2 nanowires in our previous report,[17] with peaks at 477 cm, 636 cm, and 775 cm^{-1}, some downward shift of the Eg, A1g, and B2g vibration modes for the SnO_2@carbon nanofibers could have resulted from the specific nanoscale structure, with the small SnO_2 crystals encapsulated in the carbon matrices composing the one-dimensional nanofibers.[29] The other two weak Raman peaks at 502.17 and 679.19 cm^{-1} are ascribed to the A2u mode and Eu(2) mode, respectively.[30] The appearance of these two modes in the Raman spectrum may also be related to the size effect of the particular one-dimensional nanofibers.[17,29,30] The peak at 552.45 cm^{-1}, identified as S2 mode, is believed to be the consequence of the disorder activation of the SnO_2@carbon nanofibers.[30] Figure A4(b) shows the Raman spectrum of SnO_2@carbon nanofibers between 900 and 2000 cm^{-1} and includes the fitted spectrum with two Gaussian peaks. The two peaks at 1358 and 1532 cm^{-1} are assigned to the disorder band (D band) and the graphene band (G band), respectively.[31–33] The relative intensity ratio of the D and G bands, depending on the perfection of the graphite layer structure, is also shown in Fig. A4(b) and further confirms a typical disordered carbon.

To reveal the presence and oxidation states of tin and carbon in the SnO_2@carbon nanofibers, x-ray photoelectron spectroscopy (XPS) analysis has been conducted from 0 to 1100 eV. Obvious C1s, O1s, and Sn3d peaks were detected, and their high-resolution spectra are shown in Figs. 4(a)–4(c), respectively. Figure 4(a) displays the high-resolution spectrum of the C1s region of as-prepared SnO_2@carbon nanofibers fitted to five peaks, including unoxidized graphitic (sp2) carbon. The two large peaks at 284.45 and 284.98 eV are possibly attributable to graphitic carbon containing a polyaromatic layered structure,[34,35] while the peak at 285.6 eV should probably be assigned to disordered carbon.[34] Some oxidized carbon functions are also found that result from the higher binding energy (BE) peaks at 286.68 and 288.5 eV assigned to oxidized carbon present in alcohol and carbonyl, respectively. As shown in Fig. 4(b), a pronounced O1s response occurred from 530–532 eV. A portion could come from unreduced SnO_2 as evidence by the O1s BE peak at ~530.7 eV,[34] while the peak at 531.3 eV may be the result of the OH^- radical, adsorbed oxygen, or the carbonyl.[34] As for the high BE peak at 532.2 eV, it is possibly attributable to the alcohol, which is in good accordance with the fitted C1s peaks in Fig. 4(a). The Sn3d spectrum [Fig. 4(c)] for SnO_2@carbon comprises two symmetrical peaks with BEs at 487.07 and 495.46 eV, which are attributable to Sn3d5/2 and Sn3d3/2, respectively. The separation between these two peaks is 8.39 eV, in good agreement with the energy splitting reported for SnO_2.[8,36,37] In all, the XPS results confirm that the as-prepared SnO_2@carbon nanofibers are composed of pure SnO_2 and carbon, except for some adsorbed water or OH^- on their surfaces. Additionally, part of the carbon binds with the SnO_2 by means of C–O or C=O to form this particular structure, i.e., one-dimensional SnO_2@carbon nanofibers consisting of SnO_2 particles encapsulated in carbon matrices.

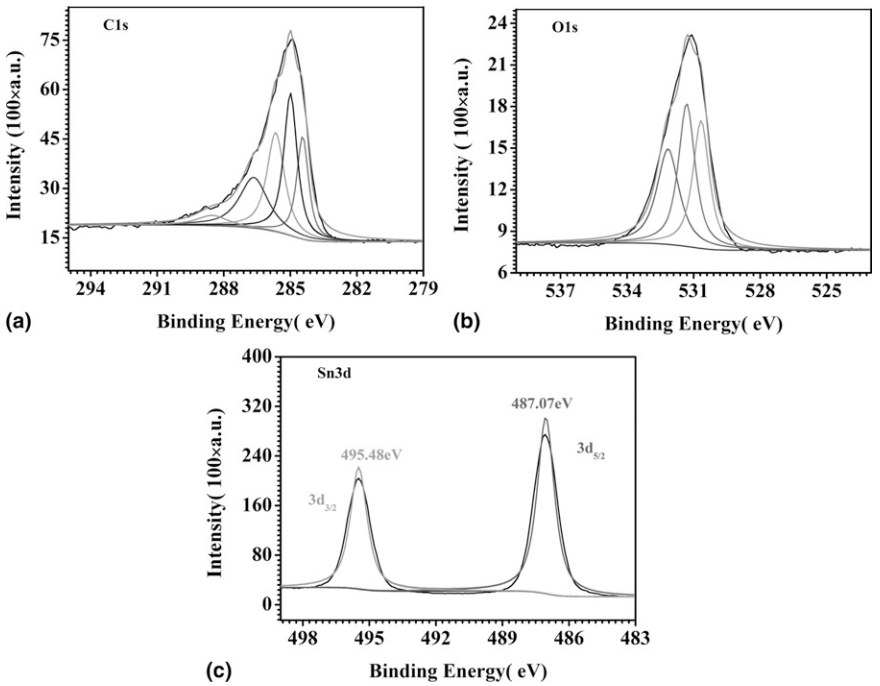

FIG. 4. XPS high-resolution spectra of (a) C1s, (b) O1s, and (c) Sn3d region of as-prepared SnO_2@carbon nanofibers.

The electrochemical performance of SnO_2@carbon nanofibers for the lithium ion battery has been characterized with the galvanostatic discharge–charge cycling and cyclic voltammetry, as shown in Fig. 5. To identify the electrochemical reactions during charge/discharge cycles, the cyclic voltammograms (CV) of SnO_2@carbon nanofibers for lithium ion battery were obtained and are presented in Fig. 5(a). The first CV profiles show two apparent reduction peaks around 0.12 and 0.873 V. The 0.873 V peak should be partly ascribed to Li_2O formation[17,38] according to the reaction

$$SnO_2 + 4Li^+ + 4e^- \Rightarrow Sn + 2Li_2O \quad . \qquad (1)$$

This peak disappeared slowly during the subsequent CV cycles, as shown in Fig. 5(a). The 0.12 V peak observed during the first discharge is attributed to the alloying of tin with lithium.[38] The evidence of both a weak reduction peak at 1.147 V, originating from the electrolyte decomposition[19] when SnO_2 nanocrystals in the SnO_2@carbon nanofibers react with Li+, and the slow disappearance of the 0.873 V peak further demonstrates that most of the SnO_2 nanoparticles in the nanofibers are encapsulated in the carbon matrices.[38] After the first CV cycle, the electrode delivers quite reversible behavior, mainly in terms of the following alloying/dealloying reactions:

$$Sn + xLi^+ + xe^- \Leftrightarrow Li_xSn(0 < x \leq 4.4) \quad . \qquad (2)$$

In the following CV cycles, three main pairs of reduction and oxidation peaks at 0.586 and 0.74 V, 0.337 and 0.638 V, and 0.136 and 0.161 V can be ascribed to the process of Li_xSn formation according to reaction (2), which is considered reversible to a large extent.[8,19,20] The other pairs of reduction and oxidation peaks at 0.784 and 1.155 V, representing the irreversible behavior according to reaction (1), did not disappear abruptly but gradually decreased in the subsequent CV cycles, mainly because of the nature of the SnO_2 nanocrystals encapsulated in the carbon matrices in the SnO_2@carbon nanofibers.

The cycling performance of SnO_2@carbon nanofiber electrode from the first cycle to the 100th cycle was obtained at a constant current of approximately 100 mA/g, with a cutoff voltage window of 0.05 to 1.5 V (versus Li/Li^+). For comparison purposes, the cycling performance of both the as-prepared SnO_2@carbon nanofibers (100 cycles) and the pure SnO_2 nanofibers (58 cycles) that were produced in our laboratory[26] are shown in Fig. 5(b). There is an obvious enhancement in the electrochemical behavior associated with encapsulation of the SnO_2 nanoparticles into the carbon matrices in the SnO_2@carbon nanofibers. The SnO_2@carbon nanofibers deliver much higher Li^+ storage and a larger initial reversible capacity of 964 mAh/g for the first cycle. Additionally, the SnO_2@carbon nanofibers display an initial coulombic efficiency of approximately 55.43%, which is obviously higher than that of the pure SnO_2 nanofibers (49.96%). Moreover, it can be clearly seen that the SnO_2@carbon nanofibers present a higher reversible capacity (420 mAh/g after 100 cycles) and better cyclic retention up to the 100th cycle while the capacity of the pure SnO_2 nanofibers decreases to 380 mAh/g after 58 cycles, as described in Fig. 5(b). To further investigate the effects of the carbon matrices that encapsulate the SnO_2 nanoparticles in the SnO_2@carbon nanofibers on the electrochemical behavior of SnO_2@carbon nanofiber electrode at different charge/discharge rates, the cycling performance from the first cycle to the 100th cycle for the SnO_2@carbon nanofibers and the pure SnO_2 nanofibers at different charge/discharge rates

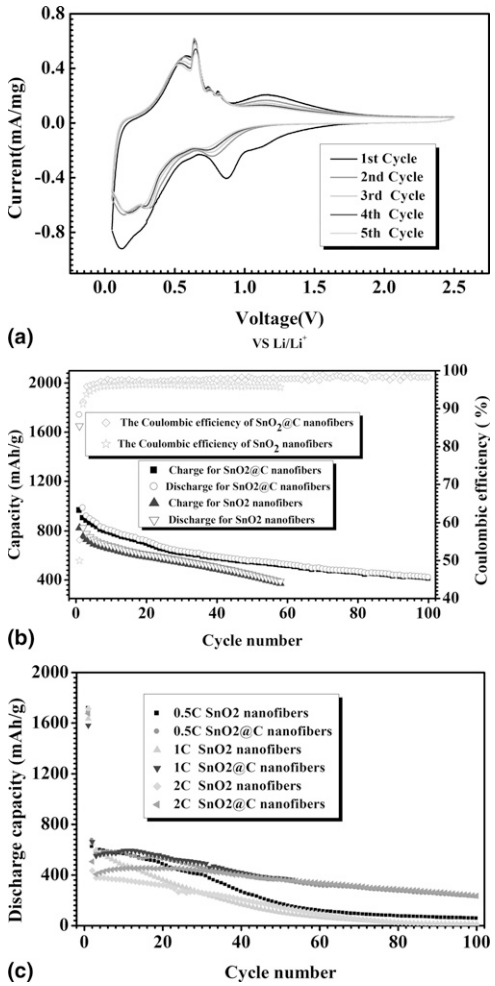

FIG. 5. (a) Cyclic voltammograms of SnO_2@carbon nanofiber electrode from the first cycle to the fifth cycle at a scan rate of 0.05 mV/s in the voltage range of 0.05–2.5 V. (b) The cycling performance from the first cycle to the 100th cycle of the SnO_2@carbon nanofibers and SnO_2 nanofibers (58 cycles) at the same current density, 100 mA/g. (c) The cycling performance from the first cycle to the 100th cycle of the SnO_2@Carbon nanofibers and SnO_2 nanofibers at different discharge rates (0.5, 1, 2 C).

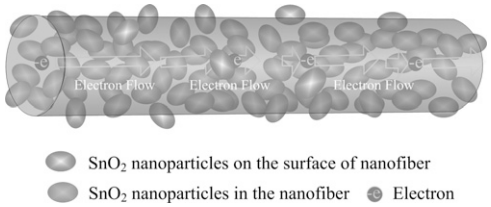

SCHEME 1. Schematic diagram showing the conductivity during the discharge/charge process as electrode.

(0.5, 1, 2 C) has been displayed in Fig. 5(c). The SnO_2@carbon nanofiber electrode delivers a rate capacity of about 226 mAh/g at 0.5 C, even after 100 cycles, and 236 mAh/g at 2 C after 100 cycles, respectively, while these values for the pure SnO_2 nanofiber electrode are only 55.8 mAh/g at 0.5 C after 100 cycles and 10.5 mAh/g at 2 C after 100 cycles. It should be noted that even though the rate capacities of the pure SnO_2 nanofiber electrode decreased to low values after 100 cycles, as shown in Fig. 5(c), the corresponding rate capacities of the SnO_2@carbon nanofiber electrode after 100 cycles are stable at more than 220 mAh/g and almost invariable with rate.

The highly improved electrochemical behavior of the SnO_2@carbon nanofiber electrode is probably attributable to its special structure with one-dimensional nanofibers consisting of SnO_2 nanoparticles encapsulated in carbon matrices. The improvement should be attributed to fewer SnO_2 nanocrystals in direct contact with the electrolyte during the charge/discharge process, as well as to the improvement in the charge transport induced by the carbon matrices in the SnO_2@carbon nanofibers, as described in Scheme 1. These carbon matrices could not only improve electronic conduction (see Scheme 1), owing to the high-speed charge pathways provided by the carbon matrix, but also increase Li^+ transport between the active phases.[8,19] Additionally, the carbon matrices encapsulating the SnO_2 nanoparticles act as a "buffer zone" to accommodate the large volume changes and prevent the agglomeration of the tin nanocrystals during charge/discharge cycling. Moreover, the nanostructured SnO_2 particles in the SnO_2@carbon nanofibers shorten the transport lengths for both electrons and lithium ions to a large extent, and the mesopores in the SnO_2@carbon nanofibers ensure a high electrode–electrolyte contact area. All these factors finally lead to not only improved reversible capacity, initial coulombic efficiency, and cyclic retention, but also to great enhancement of the rate capacity.

IV. CONCLUSIONS

We present a simple and low-cost approach to the synthesis of SnO_2@carbon composite nanofibers by a combination of electrospinning and subsequent thermal treatments in air and then in argon. The as-prepared SnO_2@carbon nanofibers, consisting of SnO_2 nanoparticles encapsulated in carbon matrices, exhibit highly improved electrochemical performance in lithium ion battery application owing to both the high conductivity pathways for electrons and lithium ions and the buffering effect provided by the carbon matrices in the nanofibers during the charge/discharge cycling. This composite nanofiber delivers a greatly improved reversible capacity of 420 mAh/g after 100 cycles at a constant current of 100 mA/g. It also exhibits strong enhancement of the reversible discharge capacity at higher rates, such as 0.5, 1, and 2 C, compared with that of the pure SnO_2 nanofibers. The rate capability of SnO_2@carbon nanofibers varies little with the current rate, partly because of the effective charge pathways formed by the carbon matrices in the nanofibers. The electrochemical behavior of SnO_2@carbon nanofiber electrode makes it a promising anode material for lithium ion batteries. Of course, there is still much room to improve the electrochemical performance of SnO_2@carbon nanofibers by optimizing the ratio of carbon matrices to the SnO_2 to reduce the number of SnO_2 crystals on the surface of the nanofibers. This will be further studied in the future.

ACKNOWLEDGMENTS

Part of the work is funded by an Australian Research Council (ARC) Linkage Grant (LP0775456), the Postdoctoral Foundation Program of Fuzhou University (BSH-0601), the Natural Science Foundation Program of Fujian Province (A0510011), and the Talents Foundation Program of Fuzhou University. The authors also would like to thank Dr. Tania Silver at the University of Wollongong for critical reading of the manuscript and Mr. Attard Darren for his great contribution. Furthermore, the authors are grateful to Dr. Sean Li at the University of New South Wales for his contributions to the XPS and Raman experiments.

REFERENCES

1. K.T. Nam, D-W. Kim, P.J. Yoo, C-Y. Chiang, N. Meethong, P.T. Hammond, Y-M. Chiang, and M.A. Belcher: Virus-enabled synthesis and assembly of nanowires for lithium ion battery electrodes. *Science* **312,** 885 (2006).
2. G.F. Ortiz, I. Hanzu, T. Djenizian, P. Lavela, J.L. Tirado, and P. Knauth: Alternative Li-ion battery electrode based on self-organized titania nanotubes. *Chem. Mater.* **21,** 63 (2009).
3. S-H. Lee, Y-H. Kim, R. Deshpande, P.A. Parilla, E. Whitney, D.T. Gillaspie, K.M. Jones, A.H. Mahan, S. Zhang, and A.C. Dillon: Reversible lithium-ion insertion in molybdenum oxide nanoparticles. *Adv. Mater.* **20,** 3627 (2008).
4. G.F. Ortiz, I. Hanzu, P. Knauth, P. Lavela, J.L. Tirado, and T. Djenizian: TiO_2 nanotubes manufactured by anodization of Ti thin films for on-chip Li-ion 2D microbatteries. *Electrochim. Acta* **54,** 4262 (2009).
5. Y. Wang, J.Y. Lee, and H.C. Zeng: Polycrystalline SnO_2 nanotubes prepared via infiltration casting of nanocrystallites and their electrochemical application. *Chem. Mater.* **17,** 3899 (2005).

6. Y. Idota, T. Kubota, A. Matsufuji, Y. Maekawa, and T. Miyasaka: Tin-based amorphous oxide: A high-capacity lithium-ion–storage material. *Science* **276,** 1395 (1997).
7. J.L. Tirado, R. Santamría, G.F. Ortiz, R. Menéndez, P. Lavela, J.M. Jiménez-Mateos, F.J. Gómez García, A. Concheso, and R. Alcántara: Tin–carbon composites as anodic material in Li-ion batteries obtained by co-pyrolysis of petroleum vacuum residue and SnO_2. *Carbon* **45,** 1396 (2007).
8. M-S. Park, Y-M. Kang, J-H. Kim, G-X. Wang, S-X. Dou, and H-K. Liu: Effects of low-temperature carbon encapsulation on the electrochemical performance of SnO_2 nanopowders. *Carbon* **46,** 35 (2008).
9. Y. Wang, H.C. Zeng, and J.Y. Lee: Highly reversible lithium storage in porous SnO_2 nanotubes with coaxially grown carbon nanotube overlayers. *Adv. Mater.* **18,** 645 (2006).
10. J. Liu, Y. Li, X. Huang, R. Ding, Y. Hu, J. Jiang, and L. Liao: Direct growth of SnO_2 nanorod array electrodes for lithium-ion batteries. *J. Mater. Chem.* **19,** 1859 (2009).
11. H. Kim and J. Cho: Hard templating synthesis of mesoporous and nanowire SnO_2 lithium battery anode materials. *J. Mater. Chem.* **18,** 771 (2008).
12. G. Chen, Z. Wang, and D. Xia: One-pot synthesis of carbon nanotube@SnO_2–Au coaxial nanocable for lithium-ion batteries with high rate capability. *Chem. Mater.* **20,** 6951 (2008).
13. H-X. Zhang, C. Feng, Y-C. Zhai, K-L. Jiang, Q-Q. Li, and S-S. Fan: Cross-stacked carbon nanotube sheets uniformly loaded with SnO_2 nanoparticles: A novel binder-free and high-capacity anode material for lithium-ion batteries. *Adv. Mater.* **21,** 2299 (2009).
14. Z. Wang, G. Chen, and D. Xia: Coating of multi-walled carbon nanotube with SnO_2 films of controlled thickness and its application for Li-ion battery. *J. Power Sources* **184,** 432 (2008).
15. N. Du, H. Zhang, B. Chen, X. Ma, X. Huang, J. Tu, and D. Yang: Synthesis of polycrystalline SnO_2 nanotubes on carbon nanotube template for anode material of lithium-ion battery. *Mater. Res. Bull.* **44,** 211 (2009).
16. M. Zheng, G. Li, X. Zhang, S. Huang, Y. Lei, and L. Zhang: Fabrication and structural characterization of large-scale uniform SnO_2 nanowire array embedded in anodic alumina membrane. *Chem. Mater.* **13,** 3859 (2001).
17. M-S. Park, G-X. Wang, Y-M. Kang, D. Wexler, S-X. Dou, and H-K. Liu: Preparation and electrochemical properties of SnO_2 nanowires for application in lithium-ion batteries. *Angew. Chem. Int. Ed.* **46,** 750 (2007).
18. P. Meduri, C. Pendyala, V. Kumar, G.U. Sumanasekera, and M.K. Sunkara: Hybrid tin oxide nanowires as stable and high capacity anodes for Li-ion batteries. *Nano Lett.* **9,** 612 (2009).
19. M-S. Park, Y-M. Kang, S-X. Dou, and H-K. Liu: Reduction-free synthesis of carbon-encapsulated SnO_2 nanowires and their superiority in electrochemical performance. *J. Phys. Chem. C* **112,** 11286 (2008).
20. X.W. Lou, D. Deng, J.Y. Lee, and L.A. Archer: Preparation of SnO_2/carbon composite hollow spheres and their lithium storage properties. *Chem. Mater.* **20,** 6562 (2008).
21. R. Demir-Cakan, Y-S. Hu, M. Antonietti, J. Maier, and M-M. Titirici: Facile one-pot synthesis of mesoporous SnO_2 microspheres via nanoparticles assembly and lithium storage properties. *Chem. Mater.* **20,** 1227 (2008).
22. Z. Ying, Q. Wan, H. Cao, Z.T. Song, and S.L. Feng: Characterization of SnO_2 nanowires as an anode material for Li-ion batteries. *Appl. Phys. Lett.* **87,** 113108 (2005).
23. D. Li and Y. Xia: Electrospinning of nanofibers: Reinventing the wheel? *Adv. Mater.* **16,** 1151 (2004).
24. C. Kim, K.S. Yang, M. Kojima, K. Yoshida, Y.J. Kim, Y.A. Kim, and M. Endo: Fabrication of electrospinning-derived carbon nanofiber webs for the anode material of lithium-ion secondary batteries. *Adv. Funct. Mater.* **16,** 2393 (2006).
25. L. Ji and X. Zhang: Electrospun carbon nanofibers containing silicon particles as an energy-storage medium. *Carbon* **47,** 3219 (2009).
26. Z. Yang, Gu. Du, C. Feng, S. Li, Z. Chen, P. Zhang, Z. Guo, X. Yu, G. Chen, and H. Liu: Synthesis of uniform polycrystalline tin dioxide nanofibers and electrochemical application in lithium ion batteries. *Nanotechnology* (under review).
27. X.W. Lou, J.S. Chen, P. Chen, and L.A. Archer: One-pot synthesis of carbon-coated SnO_2 nanocolloids with improved reversible lithium storage properties. *Chem. Mater.* **21,** 2868 (2009).
28. G. Wang, Y. Ji, X. Huang, X. Yang, P-I. Gouma, and M. Dudley: Fabrication and characterization of polycrystalline WO_3 nanofibers and their application for ammonia sensing. *J. Phys. Chem. B* **110,** 23777 (2006).
29. R.S. Ningthoujam and S.K. Kulshreshtha: Nanocrystalline SnO_2 from thermal decomposition of tin citrate crystal: Luminescence and Raman studies. *Mater. Res. Bull.* **44,** 57 (2009).
30. J.X. Wang, D.F. Liu, X.Q. Yan, H.J. Yuan, L.J. Ci, Z.P. Zhou, Y. Gao, L. Song, L.F. Liu, W.Y. Zhou, G. Wang, and S.S. Xie: Growth of SnO_2 nanowires with uniform branched structures. *Solid State Commun.* **130,** 89 (2004).
31. T. Moon, C. Kim, S-T. Hwang, and B. Park: Electrochemical properties of disordered-carbon-coated SnO_2 nanoparticles for Li rechargeable batteries. *Electrochem. Solid-State Lett.* **9**(9), A408 (2006).
32. F. Su, X.S. Zhao, Y. Wang, J. Zeng, Z. Zhou, and J.Y. Lee: Synthesis of graphitic ordered macroporous carbon with a three-dimensional interconnected pore structure for electrochemical applications. *J. Phys. Chem. B* **109,** 20200 (2005).
33. Y. Fu, R. Ma, Y. Shu, Z. Cao, and X. Ma: Preparation and characterization of SnO_2/carbon nanotube composite for lithium ion battery applications. *Mater. Lett.* **63,** 1946 (2009).
34. XPS database on Web. http://www.lasurface.com/database/elementxps.php (September 2009).
35. S.H. Lee, M. Mathews, H. Toghiani, D.O. Wipf, and C.U. Pittman: Fabrication of carbon-encapsulated mono- and bimetallic (Sn and Sn/Sb alloy) nanorods: Potential lithium-ion battery anode materials. *Chem. Mater.* **21,** 2306 (2009).
36. Y. Wang, I. Djerdj, B. Smarsly, and M. Antonietti: Antimony-doped SnO_2 nanopowders with high crystallinity for lithium-ion battery electrode. *Chem. Mater.* **21,** 3202 (2009).
37. N. Sharma, J. Plévert, S. Rao, B.V.R. Chowdari, and T.J. White: Tin oxides with hollandite structure as anodes for lithium ion batteries. *Chem. Mater.* **17,** 4700 (2005).
38. Y. Yu, L. Gu, C. Wang, A. Dhanabalan, P.A.V. Aken, and J. Maier: Encapsulation of Sn@carbon nanoparticles in bamboo-like hollow carbon nanofibers as an anode material in lithium-based batteries. *Angew. Chem. Int. Ed.* **48,** 6485 (2009).

APPENDIX

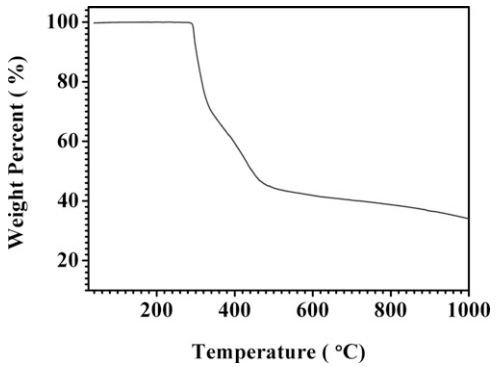

FIG. A1. TGA curve of polyacrylonitrile (PAN) in argon.

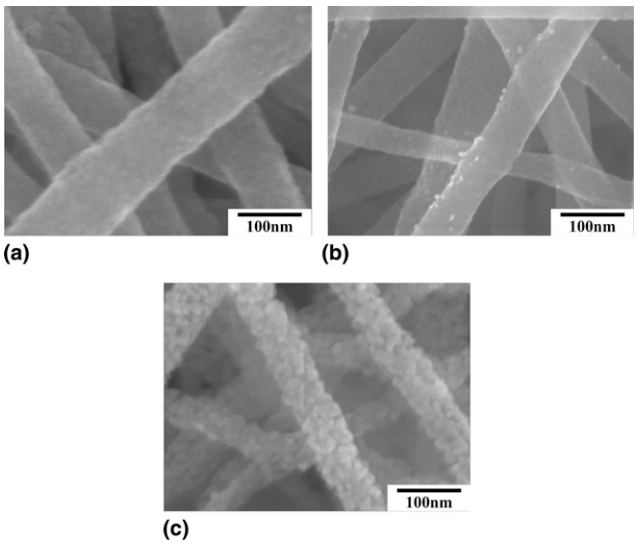

FIG. A2. High-magnification FE—SEM images of the partly pyrolyzed SnO_2 composite nanofibers, SnO_2@carbon nanofibers, and SnO_2 nanofibers: (a) high magnification FE–SEM image of partly pyrolyzed and carbonized SnO_2 composite nanofibers treated in air at 360 °C for 1 h; (b) high-magnification FE–SEM image of SnO_2@ carbon nanofibers treated in air at 360 °C for 1 h and further in argon at 500 °C for 2 h; (c) high-magnification FE–SEM image of SnO_2 nanofibers after calcination in air at 500 °C for 2 h.

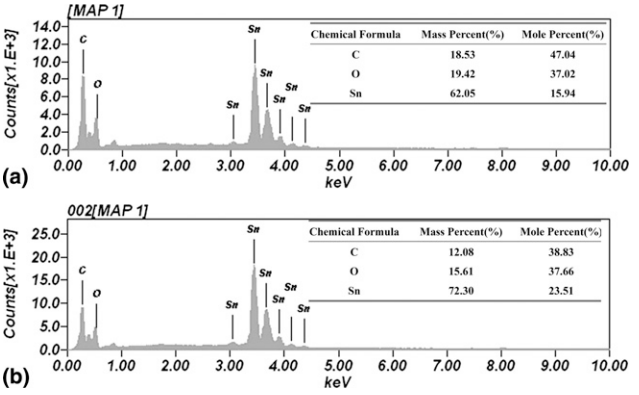

FIG. A3. Energy-dispersive x-ray (EDX) spectra of SnO_2@carbon nanofibers and corresponding content tables for the samples (inset): (a) SnO_2@carbon nanofibers treated in air at 360 °C for 1 h, (b) the SnO_2@carbon nanofibers treated in air at 360 °C for 1 h and further in argon at 500 °C for 2 h.

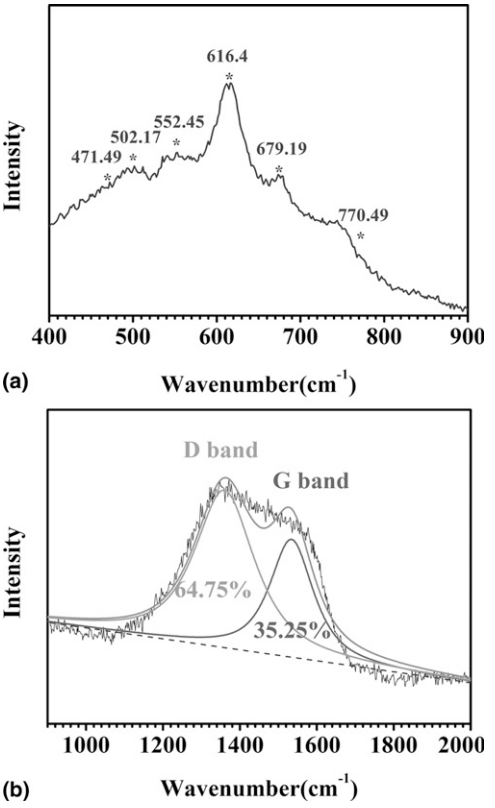

FIG. A4. Raman spectra of SnO_2@carbon nanofibers: (a) band for SnO_2; (b) band for carbon.